Wisent genome assembly uncovers extended runs of homozygosity and a large deletion that inactivates the thyroid hormone responsive gene

Chiara Bortoluzzi[1], Xena Marie Mapel[1], Stefan Neuenschwander[2], Fredi Janett[3], Hubert Pausch[1, #], Alexander S. Leonard[1, #]

Affiliations: [1]Animal Genomics, Department of Environmental Systems Science, Universitätstrasse 2, 8092 Zürich, Switzerland; [2]Animal Genetics, Department of Environmental Systems Science, Tannenstrasse 1, 8092 Zürich, Switzerland; [3]Clinic of Reproductive Medicine, Vetsuisse Faculty, University of Zürich, Winterthurerstrasse 260, 8057, Zürich, Switzerland

[#]Corresponding authors: Hubert Pausch (hubert.pausch@usys.ethz.ch), Alexander S. Leonard (alexander.leonard@usys.ethz.ch)

Abstract

The wisent (*Bison bonasus*) is Europe's largest land mammal. A restoration program established from 12 captive individuals rescued the wisent from extinction in the early 20th century. We produced a PacBio HiFi-read based assembly (GenBank accession: GCA_963879515.1) containing 99.7% of the near-universal mammalian single copy genes with a contig N50 value of 91 Mb which improves contiguity a thousand-fold over the existing draft wisent assembly. Excessive runs of homozygosity in the genome of the wisent compromised the separation of the HiFi reads into parental-specific read sets, which resulted in inferior haplotype assemblies. A bovine super-pangenome built with assemblies from wisent, bison, gaur, yak, taurine and indicine cattle identified a 1,580 bp deletion removing the entire protein-coding sequence of *THRSP* encoding thyroid hormone-responsive protein from the wisent and bison genomes. Analysis of 725 whole genome sequenced samples across the *Bovinae* subfamily showed that the deletion is fixed in *Bison* but absent in *Bos* and *Bubalus*. Transcriptomic data revealed that the *THRSP* transcript is highly abundant in adipose, fat, liver, muscle, and mammary gland tissue of *Bos* and *Bubalus,* but absent in *Bison* indicating that the deletion inactivates *THRSP* which might contribute to low milk and meat fat content observed in *Bison*. Our findings demonstrate that super-pangenomes can reveal potentially trait-associated variation across phylogenies, but also emphasize that haplotype assemblies from species that went through population bottlenecks warrant scrutiny, as they may have accumulated long runs of homozygosity that complicate phasing.

Keywords: *Bison bonasus,* wisent, endangered species, long read sequencing, trio-binning, genome assembly, gene loss, pangenomics

Introduction

The wisent (*Bison bonasus*), also known as the European bison, is a member of the *Bovidae* family that contains several domesticated livestock species, such as cattle, buffalo, yak, sheep, and goat (Chen et al., 2019). The wisent went extinct in the wild in 1921. A restoration program established in 1942 from 12 captive individuals by the International Society for the Preservation of the European Bison led to the creation of the lowland and lowland-Caucasian lines, which are still managed as separate populations (Bont, 2017; Tokarska et al., 2011). As a result of these efforts, the wild wisent population has expanded to around 6,800 free-roaming individuals across 10 countries (Plumb, 2022). However, the wisent is still considered a near threatened species according to the International Union for the Conservation of Nature (Olech and Perzanowski, 2022).

Wisent genetic research had long relied on mitochondrial genome sequences and microsatellite markers (Soubrier et al., 2016; Tokarska et al., 2011, 2009). More recent investigations into genome-wide genetic diversity in wisent have utilized a taurine cattle (*Bos taurus taurus*) reference genome and bovine microarrays (Druet et al., 2020; Gautier et al., 2016; Wojciechowska et al., 2023). Considering that wisent and taurine cattle diverged between 1.7 and 0.85 million years before present (Gautier et al., 2016), this methodological approach likely introduces reference bias (Chen et al., 2021; Günther and Nettelblad, 2019). Low contiguity (contig N50: 14.53 Kb; scaffold N50: 4.69 Mb) and high fragmentation (29,074 scaffolds) of a short read-based wisent assembly (Wang et al., 2017) complicate its wider application for genetic investigations (Thomma et al., 2016), therefore assembling the wisent genome with more recent approaches is warranted. A highly contiguous genome assembly of the wisent is also of great interest for the Bovine Pangenome Consortium (Smith et al., 2023) to investigate signatures of domestication, natural and artificial selection in the genomes of divergent lineages of the *Bovinae* subfamily.

The semi-automated construction of highly contiguous, near complete, and near error-free assemblies is feasible with current sequencing and assembly methods (Jarvis et al., 2022). Trio binning is a widely used assembly method when parent-offspring trios are accessible (Cheng et al., 2021; Koren et al., 2018; Leonard et al., 2022; Rice et al., 2020; Stroupe et al., 2023). The availability of parental sequencing data allows to bin the offspring's sequencing reads into haplotype-specific sets based on

k-mers specific to either the paternal or maternal haplotype, thereby assembling maternal and paternal haplotypes (Cheng et al., 2021; Koren et al., 2018).

Here, we assemble a wisent genome with Pacific Biosciences (PacBio) HiFi data. We produce two haplotype assemblies with trio binning and a primary assembly. We show that the wisent genome contains many long runs of homozygosity (ROH), which complicates phasing and results in incomplete haplotype-resolved assemblies. We integrate the primary wisent assembly into a bovine super-pangenome and identify a putatively trait-associated deletion of the entire protein-coding sequence of *THRSP* which is fixed in wisent and bison populations.

Results and Discussion

Assembly of the wisent genome

A draft reference of the wisent genome was previously assembled with short sequencing reads (Wang et al., 2017) but the assembly is highly fragmented and therefore not suitable for detailed pangenome analyses (Tonkin-Hill et al., 2020). To make the wisent genome amenable to pangenome analyses, such as identifying structural variants differing between wisent and other wild and domesticated members of the *Bovinae* subfamily, we sampled tissue from a parent-offspring trio to assemble the wisent genome with long reads through trio binning. We collected 131.1 Gb (or approximately 44x coverage) of HiFi reads, with a mean read length of 19.3 Kb and a mean quality value of 32.4 from a male wisent (hereafter referred to as F1) from a captive population. We further collected approximately 40x, 38x, and 36x coverage of Illumina short reads from the F1, his sire, and dam, respectively. We used the parental short reads to trio-bin the long reads, assigning an unknown/paternal/maternal tag to each read. Overall, the "binnability" of the wisent sample reads was 61.9%, which is low compared to the 79.9%, 85.0%, or 99.2% binnability observed for intra-breed (Braunvieh x Braunvieh) (Leonard et al., 2024), inter-breed (Rätisches Grauvieh x Simmental) (Milia et al., 2024), or inter-subspecies (Nellore x Brown Swiss [indicine x taurine]) (Leonard et al., 2022) *Bos taurus* crosses (**Fig. 1a-d**). The F1 sample also had higher variability in binnability along the genome than observed previously in other bovines, suggesting that in this wisent trio there is less parental-specific sequence used to assign haplotype, but also a more uneven distribution of such sequence (**Fig. 1e; Supplementary Fig. 1**).

Regions with high proportions of unassigned reads can safely be treated as homozygous sequences present in both offspring haplotypes. However, regions with moderate levels of unassigned reads and high levels of reads assigned to a single haplotype can introduce an assembly gap in the unrepresented

haplotype and likely lead to assembly errors - due to mixing of haplotypes - in the overrepresented haplotype. There was a dam/sire-assigned read bias greater than 5-fold for 213 100-Kb bins in the F1 sample, over three times greater than observed in a previously analyzed *Bos taurus taurus* intra-breed (Braunvieh x Braunvieh) F1 sample with only 70 bins with large imbalances (**Fig. 1f**).

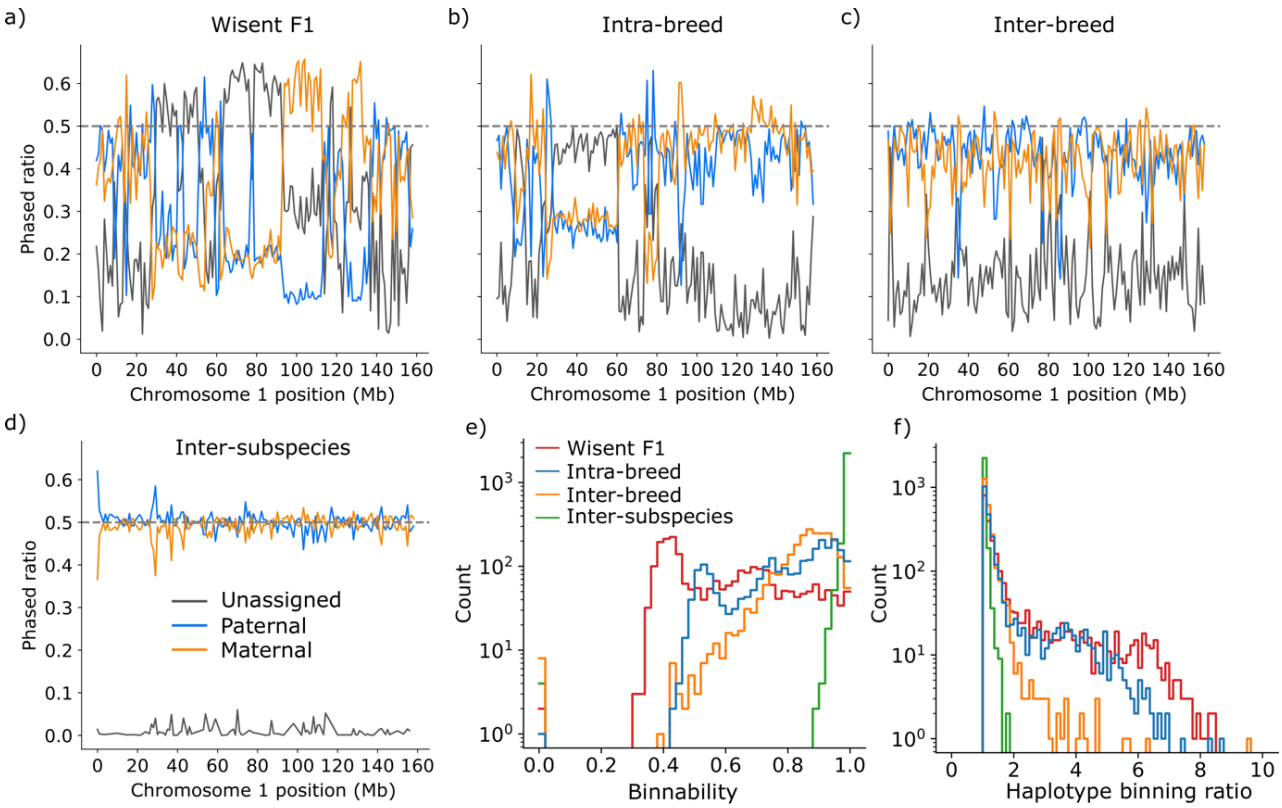

Figure 1. Trio binning of the wisent *(Bison bonasus)* genome. (**a-d**) Fraction of reads per 100 Kb window tagged as unassigned, paternal, or maternal haplotypes across chromosome 1 for the Wisent sample, an intra-breed sample (BSWxBSW), and inter-breed sample (RGVxSIM), and an inter-subspecies sample (NELxBSW). (**e**) Histogram of proportion of parental-assigned reads (paternal + maternal)/total) per window across all autosomes. Proportions close to 1 indicate unambiguous phasing. (**f**) Histogram of paternal assigned read ratio (paternal/maternal if paternal > maternal else maternal/paternal) per window across all autosomes. Values close to 1 indicate balanced phasing, while higher values indicate either paternal or maternal reads are disproportionately assigned.

Given the low binnability and biased assignment of parental reads in the F1 sample, we used hifiasm to generate both a primary (collapsed) assembly, as well as two haplotype-resolved assemblies, to examine the impact of assembler phasing assumptions. We calculated contiguity, correctness, and completeness for all three new assemblies, as well as the existing short-read based draft wisent reference genome (Wang et al., 2017). Most metrics demonstrate the outstanding quality of our assemblies, with the primary assembly improving contiguity a thousand-fold over the existing draft

wisent assembly (**Table 1**). As a result, both haplotypes and primary assembly captured a higher fraction of unassembled genome, for an additional 0.3 Gb and 0.5 Gb, respectively, while reducing the number of N bases from 125 Mb in the draft to 0.05 Mb in the primary assembly**.** Assembly completeness was estimated using compleasm and the set of 9,226 highly conserved mammalian genes. The draft and primary assembly had high completeness scores (99.0% vs 99.7%), similar to those of other cetartiodactyla high-quality assemblies (**Supplementary Table 3)**. While the contiguity and correctness of the haplotype-resolved assemblies was comparable to the primary assembly, the gene completeness was noticeably lower, especially for the maternal haplotype at 89.5%. Many of the BUSCO genes missing from one haplotype were found in either the other haplotype or the primary assembly, suggesting that the diploid sequence was incorrectly assigned to only a single haplotype. We confirmed the sporadically missing BUSCOs should have been in large regions (> Mb) of missing syntenic sequence (**Supplementary Fig. 2**), rather than local mis-assemblies disrupting BUSCO identification.

Table 1. Assembly statistics of the wisent draft assembly of (Wang et al., 2017), the two haplotype-phased assemblies, and the primary assembly generated in this study.

		Draft	**Haplotype 1 (paternal)**	**Haplotype 2 (maternal)**	**Primary**
Assembly accession		(Wang et al. 2017)	This study	This study	GCA_963879515.1 (This study)
Assembled genome size (Gb)		2.57	2.83	2.86	3.07
Number of contigs		243,242	486	480	248
Contig N50 (Mb)		0.02	74	59	91
Number of scaffolds		29,074	402	338	210
Scaffold N50 (Mb)		4.0	95	105	105
Quality Value		-	55.6	55.7	56.4
Largest scaffold (Mb)		31.6	164.4	164.1	163.9
Compleasm (%)	Complete	99.0	94.5	89.5	99.7
	Single copy	98.4	93.4	88.4	98.5
	Duplicated	0.6	1.1	1.1	1.2
	Fragmented	0.7	0.3	0.3	0.2
	Missing	0.3	5.3	10.2	0.1

Extended runs of homozygosity complicate haplotype phasing

The differences in sequence and gene content observed between the haplotype assemblies and the primary assembly were surprising, as we did not observe such a pattern in other bovine assemblies constructed earlier through trio binning (Leonard et al., 2022) and so prompted a detailed investigation. We looked at the distribution and location of regions with lower-than-expected heterozygosity (runs of homozygosity – ROH) by aligning short-reads of the F1 to the primary wisent assembly to examine whether excessive ROH had an impact on the assembly construction. Variants called from these alignments revealed that ROH covered a total of 1,383 Mb in the F1 genome corresponding to a genomic inbreeding coefficient (F_{ROH}) of 0.52 **(Fig. 2a; Supplementary Table 4).** Of these, 139 were longer than 2 Mb and tended to correspond with large regions of missing sequence in the haplotype assemblies, which appeared to derive from the hifiasm unitig graph, where unbalanced assignment of paternal phases lead to incorrect haplotype separation (**Supplementary Fig. 2**). Although many of the ROH were correctly assembled, it was striking to observe such a correspondence between regions of lower-than-expected heterozygosity and regions that are difficult to resolve in the assembly using a trio binning approach. Given the high binning variability of the wisent F1, using a bin-first-then-assemble method encounters similar haplotype-resolved assembly issues (**Supplementary Table 5**), partially improving BUSCO score (although some previously missing loci are still missing, including the region from **Supplementary Fig. 2**), but considerably worsening the haplotype switch rate and contiguity.

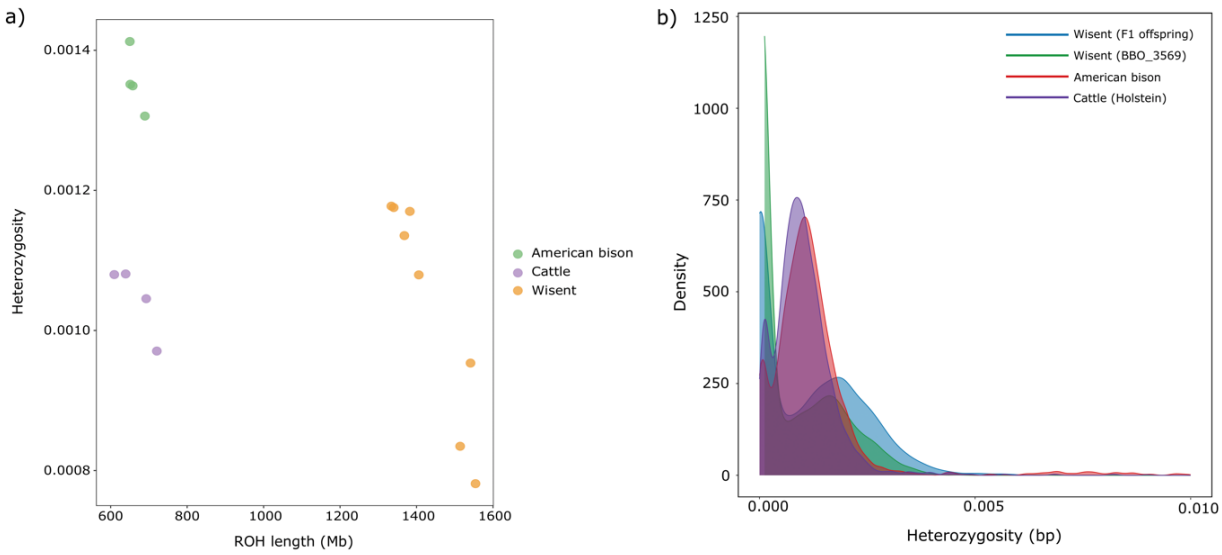

Figure 2. Genome-wide heterozygosity and runs of homozygosity. (a) Total length of runs of homozygosity (ROH) versus genome-wide heterozygosity in each wisent (*n* = 8), American bison (*n* = 4), and taurine cattle (*n* = 4) sample. **(b)** Distribution of heterozygosity in windows of 1 Mb in the F1 offspring used in the assembly construction, a wild wisent individual (BBO_3569), an American bison, and a domestic cattle breed (Holstein).

ROH covered a large fraction of the genome also in the seven (5 captive, 2 wild) additional wisents we investigated (**Fig. 2a; Supplementary Table 4**). On average, 1,437 Mb of their genomes were in ROH resulting in a F_{ROH} of 0.56. Between 121 and 168 ROH longer than 2 Mb were observed in the eight wisents studied. These long homozygous regions likely reflect founder effects resulting from the genetic bottleneck and expansion of the wisent population at the beginning of the 20th century (Gautier et al., 2016). Compared to the wisent samples, we found fewer ROH in the American bisons and taurine cattle covering only a quarter of their genomes (American bison: 662 Mb; taurine cattle: 665 Mb) (**Fig. 2a).** ROH longer than 2 Mb were eight- and two-fold less abundant in American bison and cattle, respectively (**Fig. 2b).** A relatively low F_{ROH} value in American bison is likely the result of hybridization with various domestic cattle breeds, which has been encouraged since the late 1800's, when most of the surviving bison individuals were maintained by cattle ranchers in private herds (Stroupe et al., 2022).

In line with previous studies (Druet et al., 2020; Gautier et al., 2016), we observed that the genome-wide heterozygosity in the wisent ($1.04 \pm 0.16 \times 10^{-3}$) was similar to that of cattle ($1.04 \pm 0.22 \times 10^{-3}$) but lower than in American bison ($1.35 \pm 0.19 \times 10^{-3}$). However, heterozygosity varied strongly along the genome as evidenced by an excess of regions with almost no heterozygous sites (**Fig. 2b**). These findings corroborate that genome-wide heterozygosity levels are unable to reflect demographic effects that can lead to extended segments of homozygosity and are therefore of limited utility to assess variability of populations (Bosse and van Loon, 2022). Moreover, our findings emphasize that the average genome-wide heterozygosity can be a misleading metric for haplotype-resolved analyses.

Repeat and gene content of the wisent assembly

The high accuracy of HiFi reads has previously been shown to benefit the assembly of repetitive sequence (Chu et al., 2021), and so we investigate the repeat content in the new wisent assembly. Since all examined metrics provide confidence that the primary wisent assembly is highly contiguous and near complete, we used it for all downstream analyses. Repetitive elements were identified and classified using a wisent-specific *de novo* repeat library constructed with RepeatModeler. This approach led to a total repeat content in the wisent genome of 48.90%, which was similar to that of the draft assembly (47.30%), American bison (43.52%), and domestic taurine cattle (41.73%) when equally using a species-specific *de novo* repeat library (**Supplementary Table 6**). Within the first class of transposable elements (TEs), also called retrotransposons, LINEs (27.76%) were the most abundant type, which is also in agreement with their prevalence in the bovine genome (Adelson et al., 2009), followed by LTRs (4.44%) and SINEs (3.82%). We found that satellite DNA was substantially higher in

the HiFi-based wisent (9.69%) than in American bison (2.04%) and cattle (0.07%). Unclassified repeats made up just 0.85% of the wisent repeat content. While this value was similar to that of the American bison (0.88%), it was 11-fold larger than in domestic cattle (0.08%). We ran another round of repeat masking on the American bison and cattle genome using the wisent-specific repeat library generated with RepeatModeler to test the impact of the repeat library. We found that the overall repeat content did not change significantly when using either a species-specific (American bison: 43.52%; cattle: 41.73%) or a wisent-specific repeat library (American bison: 43.27%; cattle: 41.90%), suggesting that *de novo* repeat libraries are not sensitive enough to identify *de novo* repeats in highly similar genomes (1% divergence between wisent and bison and wisent and cattle) due to the levels of noise **(Supplementary Table 6**).

We performed a Kimura distance-based copy divergence analysis of TEs in the wisent assembly to estimate the age of TEs. We observed a predominance of young LINEs and LTRs, as evident from their clustering on the left side of the graph, which indicates minimal deviation from the consensus sequence (**Fig. 3a)**. Additionally, the wisent exhibited the presence of unidentified young repeat copies, classified as "unknown" in the graph. LINEs and LTRs were also the most abundant type of ancient or degenerated TEs, as indicated by their clustering on the right side of the graph.

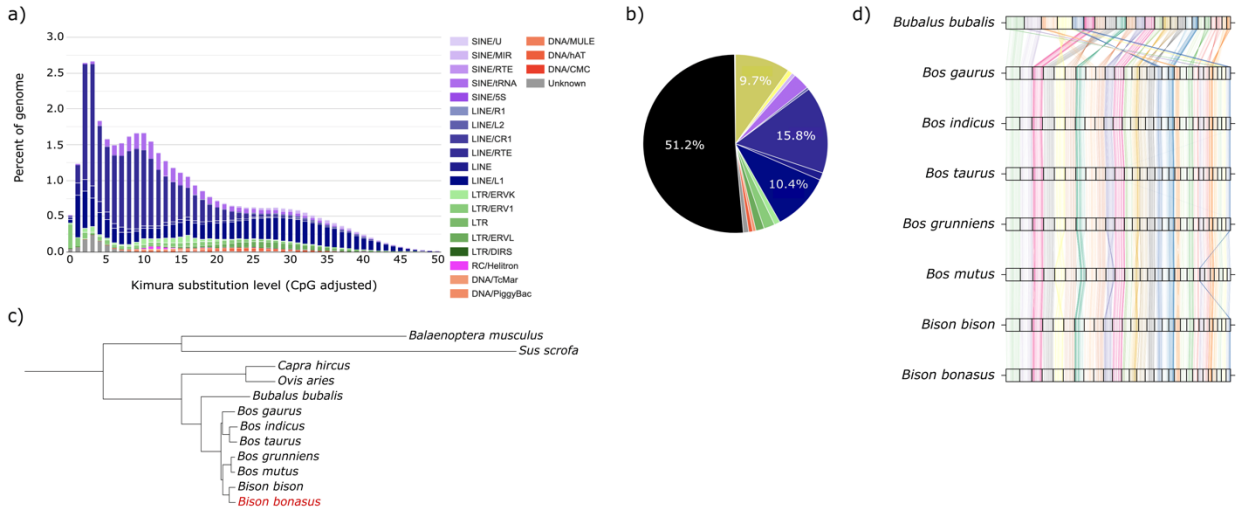

Figure 3. Primary assembly of the wisent (*Bison bonasus*). (a) Kimura substitution levels between the repeat consensus and its copies. The histogram plot shows the age distribution of transposable elements (TEs). As shown on the x-axis, the total amount of DNA in each TE class was split into bins of 5% Kimura divergence. (**b)** Pie chart representing the percentage of the genome in different repeats. The % of unmasked genome is colored in black. **(c)** Phylogenetic tree of 12 cetartiodactyla species (wisent included) as constructed from single copy BUSCO genes identified in compleasm. The phylogenetic tree was rooted on the node separating the domestic pig and blue whale from the remaining species. All nodes are fully supported. **(d)** Synteny plot showing the conservation of large-scale gene linkage and gene order across 8 species. The conserved unique single copy mammalian

genes are connected by lines according to their chromosomal location. Species are ordered following the phylogenetic tree.

We used BUSCO genes shared between the wisent and 11 cetartiodactyla species to build a phylogenetic tree (**Fig. 3c**). The wisent formed a clade with the American bison and this clade was sister to the domestic (*Bos grunniens*) and wild yak (*Bos mutus*) clade. The domestic taurine (*Bos taurus taurus*) and indicine (*Bos taurus indicus*) cattle formed a clade of their own, with the gaur (*Bos gaurus*) acting as an outgroup corroborating an earlier phylogenic reconstruction of the Bovinae subfamily (Wu et al., 2018). As expected, the water buffalo (*Bubalus bubalis*) was the most outgroup species. BUSCO genes were also used to perform a synteny analysis to investigate how gene order has changed during the evolution of species within the *Bovinae* subfamily. We found gene order to be conserved between wisent, *Bison* and various *Bos* species (**Fig. 3d**). When looking at more distantly related species, such as the water buffalo (*Bubalus bubalis*), we observed several rearrangements, as shown by the break of gene order **(Fig. 3d).**

Pangenome analysis reveals a *Bison*-specific deletion inactivating *THRSP*

We then built per-autosome super-pangenomes with the five *Bos* and two *Bison* assemblies (excluding *Bubalus bubalis* due to the different assembled karyotype [*Bos gaurus* has a Robertsonian translocation between chromosomes 1 and 29 (Mastromonaco et al., 2004) but was not assembled through the centromere fusion, leaving 29 separate assembled chromosomes]) to assess SV diversity (**Fig. 4a**). We find the wisent sample contains 74,770 SVs (insertions: 37,814, deletions: 36,956) relative to *Bos taurus taurus*, matching previous findings for other distantly related bovids (Crysnanto et al., 2021; Leonard et al., 2023). We find many SVs private to either the American bison or wisent, contrasting to wild or domestic yak which have fewer private SVs, as expected given the more recent split of yak. Using pair-wise overlap of SVs, we can infer a relationship tree (**Fig. 4b**), closely matching the more rigorously constructed phylogeny discussed previously (**Fig. 3c**), demonstrating that SVs also reflect evolutionary histories and are a rich source of variation to analyze.

We find 12,217 SVs uniquely common to *Bison* (i.e., American bison and wisent), including 96 that are predicted to have a high impact on proteins (**Supplementary File 1**). Among them, a 1,580 bp deletion which entirely overlaps the coding sequence of *THRSP* encoding thyroid hormone-responsive protein. *THRSP* has two exons, of which the first contains protein-coding sequence and the second is non-coding. The deletion is predicted to remove the protein-coding exon of *THRSP* in the two American bison and wisent haplotypes that were integrated into the pangenome (**Fig. 4c**, **Supplementary Fig 3a**). This deletion occurs in the homozygous state in all short read-sequenced bisons (n = 19) and

wisents (n = 20) we investigated, indicating it is likely fixed in both *Bison* species (**Fig. 4d**, **Supplementary Fig 3b**). The 1,580 bp deletion was neither detected in the *Bos taurus*, *Bos gaurus*, *Bos mutus* and *Bos grunniens* assemblies, nor in any of the short-read sequenced *Bos taurus taurus* and *Bos taurus indicus* (n = 674) and *Bubalus bubalis* (n = 12) samples indicating that the deletion occurred in a common ancestor of bison and wisent, after divergence from the other species of the *Bovinae* subfamily, while the 1,580 bp insertion (relative to wisent and bison) is the ancestral state. Genetic drift or selective advantages may have led to the fixation of the deletion in wisent and bison.

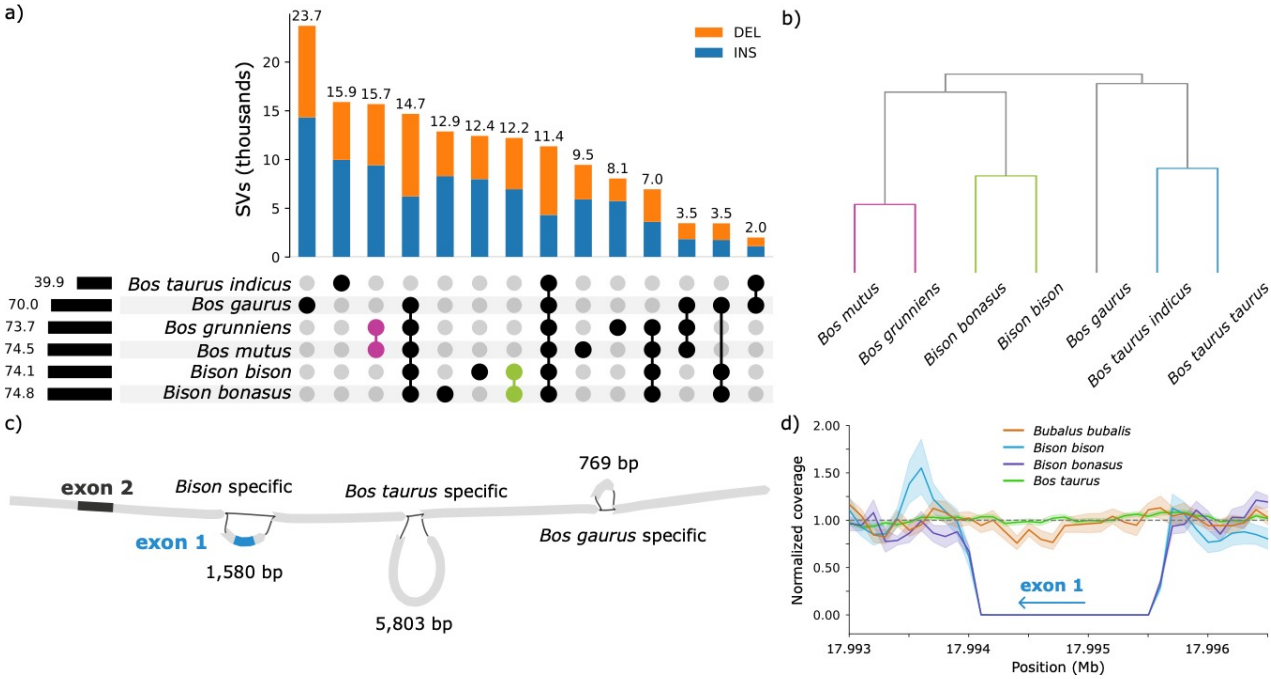

Figure 4. Structural variant analysis from seven-assembly pangenome. **(a)** UpSet plot of SVs called from the 29 autosomes. **(b)** Relationship tree inferred from pair-wise overlaps of SVs. Assemblies are correctly grouped into yak (purple), bison (green), and cattle (blue) clades. **(c)** A 1,580 bp deletion that includes the first coding exon of the *THRSP* gene was detected in the wisent and bison assemblies. **(d)** Normalized coverage of short read-sequenced data in wisent (n = 20), bison (n = 19), cattle (n = 674), and water buffalo (n = 12) samples with at least 5-fold coverage around the 1,580 bp deletion. Error bars represent the 95% confidence intervals, and the dashed line indicates the expected normalized coverage of 1.

We lifted the *THRSP* gene annotation from the *Bos taurus taurus* assembly (ARS-UCD1.2) to the haplotype-resolved, primary, and draft assemblies of wisent, finding alignment of the non-coding second exon in the paternal haplotype and primary assembly. We confirm that the partial *THRSP* gene is contained within a previously reported synteny group corroborating this region is evolutionarily highly conserved and likely under similar transcriptional regulation and function across species (Wang et al., 2004). As expected, given the deletion uncovered from the pangenome, and in line with a partial

alignment of *THRSP* in a highly contiguous American bison assembly (Oppenheimer et al., 2021) and the missing *THRSP* gene in the highly fragmented American bison reference assembly (GenBank accession: GCA_000754665.1) (Dobson et al., 2021), the coding exon was missing in the primary wisent assembly. The liftover of the coding and non-coding *THRSP* exons was not successful for the previous draft assembly and the maternal haplotype assembly, demonstrating the utility of our near-complete and highly contiguous primary assembly for genomic investigations.

The amino acid sequence of *THRSP* is evolutionarily highly conserved (**Supplementary Fig. 3d)**. The expression of *THRSP* varies across tissues but it is elevated in tissues that synthesize fatty acids (Kuemmerle and Kinlaw, 2011). Comprehensive transcriptomic data from the cattle Genotype-Tissue Expression (GTEx) project (Liu et al., 2022) confirm that *THRSP* is highly expressed in adipose tissue (5351 TPM), intramuscular fat (66 TPM), liver (34 TPM), muscle (33 TPM) and lactating mammary gland (14 TPM) of cattle (**Supplementary Fig. 3c**). We hypothesized that deletion of the first exon including the entire protein-coding sequence in wisent and bison represents a functional knock-out of *THRSP*. Transcriptomic data are not available for wisent but bison RNA-seq data are publicly available for liver, spleen, lung, skeletal muscle, kidney and supramammary lymph node tissues (Dobson et al., 2021). We mapped the bison transcriptomes to the *Bos taurus taurus* reference sequence and, as expected given the deletion, did not detect expression of the coding exon of *THRSP* (**Supplementary Fig. 3e**). Interestingly, the non-coding second exon was also not expressed in any of the bison tissues, although it is not affected by the deletion. We then aligned 73 transcriptomic data from 19 tissues from 4 water buffaloes (Si et al., 2023) against the *Bos taurus taurus* reference sequence. Water buffalo is substantially more diverged from cattle than wisent and bison, but the expression profile of both *THRSP* exons was similar to cattle with the highest transcript abundance in adipose tissue (9,776 TPM), mammary gland (1,570 TPM), skin (440 TPM), liver (298 TPM), and skeletal muscle (37 TPM) (**Supplementary Fig. 3e)**. These findings show that the non-coding exon doesn't produce mRNA in bison which supports that the deletion of the coding first exon inactivates *THRSP* and that bison and wisent are lacking the thyroid hormone-responsive protein.

Given the crucial contribution of THRSP in lipogenesis and fatty acid synthesis in the mammary gland and other tissues (Colbert et al., 2010; Kuemmerle and Kinlaw, 2011; LaFave et al., 2006), we suspect that lack of THRSP impacts the lipid metabolism in the two *Bison* species. Mice lacking THRSP produce milk with significantly less medium-chain fatty acids resulting from a decreased lipogenesis in the mammary gland (LaFave et al., 2006). Neither bison nor wisent have been domesticated, and so the composition of their milk has not been investigated. However, bison meat has lower fat than beef

(Cordain et al., 2002; Rule et al., 2002) which agrees with reduced accumulation of fat in adult *THRSP* knockout mice (Anderson et al., 2009). While *THRSP* mRNA expression in skeletal muscle tissue is correlated with intramuscular fat content in crossbred cattle (Wang et al., 2009), the precise function of THRSP in the deposition of intramuscular fat remains to be elucidated (Schering et al., 2017). Bison and wisent appear as intriguing model organisms to study the impact of missing THRSP on transcriptional changes in lipid metabolism pathways and investigate a possible causal relationship between *THRSP* expression and fat accumulation. Hybridization between *Bison* and domestic cattle which have a functional *THRSP* gene is relatively common (Koch et al., 1995), and so the phenotypic and genetic diversity of the offspring can be exploited to investigate functional consequences arising from lack of THRSP in natural knockouts.

Materials and Methods

Ethics statement

No animals were sampled for this study. No ethics approval was required for this study.

Sample selection

Blood samples of six captive wisents were provided by the Bern animal park and Langenberg animal park in Switzerland, respectively **(Supplementary Table 1).** Blood samples of five wisents were collected prior to our study for the purpose of establishing a biobank at the animal park. Another blood sample was collected from one wisent after it was killed. The decision to kill the animal was independent from our study. High-molecular weight DNA was extracted from blood using the Qiagen MagAttract HMW DNA Kit.

Long-read (Pacific Biosciences) and short-read (Illumina) sequencing

A DNA sample from a male wisent (F1) was used for PacBio HiFi sequencing. DNA fragment length and quality were assessed with the Femto Pulse system (Agilent). A HiFi library was prepared and sequenced on three SMRT cells 8M with a Sequel IIe. We also used an Illumina NovaSeq 6000 machine to generate paired end (2 x 150 bp) reads from DNA extracted from all wisents including the F1 and its parents.

Genome assembly

The wisent F1 HiFi reads were assembled with hifiasm v0.19.5 (Cheng et al., 2021) using default parameters and "-a 5 -n 5 --primary" to produce a primary assembly. We reran hifiasm without the

primary flag and instead provided parental *k*-mer databases that were created with yak v0.1 (https://github.com/lh3/yak) from parental short reads to produce two haplotype-resolved assemblies. The contig outputs were then scaffolded to the ARS-UCD2.0 *Bos taurus taurus* reference genome (GenBank assembly accession: GCA_002263795.4) with RagTag v2.1.0 (Alonge et al., 2022) primarily to orient and assign chromosome identifiers.

Assembly validation and completeness

We assessed assembly base-level quality and phasing blocks with merqury (6b5405) (Rhie et al., 2020) using meryl (https://github.com/marbl/meryl) *k*-mer databases created from parental and offspring short read sequencing. We used calN50.js (https://github.com/lh3/calN50) to evaluate the contig contiguity. We ran compleasm v0.2 (Huang and Li, 2023) using the *mammalia_odb10* database, which contains 9,226 highly conserved genes from 24 species. The hifiasm-processed unitig graph was visualized with bandageNG v2022.9 (Wick et al., 2015).

Analysis of haplotype specific F1 reads

We used canu v2.2 (Koren et al., 2017) to assign paternal/maternal/unknown haplotypes to each read, using parental *k*-mer databases created from Illumina reads with meryl v1.3. Tagged reads were then aligned with minimap2 v2.26 (Li, 2018) using the map-hifi preset to the ARS-UCD2.0 *Bos taurus taurus* reference genome. The alignments were sorted with SAMtools v1.19.2 (Li et al., 2009) and the starting coordinate for every primary alignment was recorded for each haplotype tag. We used a 100 Kb window to bin the read counts for each haplotype across the autosomes. We estimated *k*-mer distributions by creating *k*-mer databases and histograms with meryl v1.3 from each individual's HiFi reads. Sample information is given in **Supplementary Table 2**.

Repetitive sequence analysis

We generated a wisent-specific *de novo* repeat library for the primary assembly using RepeatModeler v2.0.4 (Flynn et al., 2020) to identify, classify, and mask repetitive elements. RepeatModeler was run in combination with RECON v1.08 (Bao and Eddy, 2002), RepeatScout v1.0.6 (Price et al., 2005), and Tandem Repeats Finder v4.09.1 (Benson, 1999). The complete Dfam v3.7 (Wheeler et al., 2013) and RepBase (final version 10/26/2018) (Bao et al., 2015) libraries were used to classify repetitive elements based on homology in different repeat families. Consensus sequences obtained from RepeatModeler were used to softmask the genome with RepeatMasker v4.1.5 (https://www.repeatmasker.org/). We ran RepeatMasker by specifying the *rmblast* search engine and the slow search mode. We used the *calcDivergenceFromAlign.pl* script provided by RepeatMasker to summarize the Kimura substitution

levels between the repeat consensus and its copies. Repeat landscape plots were produced with the *createRepeatLandscape.pl* script bundled in RepeatMasker. We applied this approach also to the American bison (*Bison bison*) (GenBank assembly accession: GCA_030254855.1) and taurine cattle (*Bos taurus taurus*) (GenBank assembly accession: GCA_002263795.3) assemblies for comparison purposes.

Phylogenetic tree construction

We constructed a phylogenetic tree from complete single copy orthologs identified by compleasm v0.2 (Bortoluzzi et al., 2023). We ran compleasm using the *mammalia_odb10* database on an additional set of eleven cetartiodactyla species (**Supplementary Table 3**).

We aligned the protein sequence of the 8,392 complete single copy genes shared between wisent and 11 cetartiodactyla species using MAFFT v7.490 (Katoh and Standley, 2013). Protein sequence alignments were trimmed using trimAl v1.4 (Capella-Gutiérrez et al., 2009), specifying a gap threshold of 0.8 and a minimum average similarity of 0.001. Trimmed protein sequences were concatenated to form a supermatrix, which was provided to RaxML v8.2.12 (Stamatakis, 2014) to reconstruct a maximum likelihood phylogeny. RaxML was run with the PROTGAMMAJTT model and 1,000 bootstrap replicates.

Synteny

Synteny was identified using the Chromosomal Orthologous Link analysis approach (https://github.com/chulbioinfo/chrorthlink). We used the set of complete single copy mammalian genes identified with compleasm v0.2 that were used in the phylogenetic tree analysis to assess the conservation of large-scale gene linkage and gene order compared to that of seven other members of the Bovidae family (American bison, wild yak, domestic yak, taurine cattle, indicine cattle, gaur, and water buffalo). Synteny plots were generated in R v4.2.2 using the genoPlotR library (Guy et al., 2010).

Annotation of the wisent assemblies

We used liftoff v1.6.3 (Shumate and Salzberg, 2021) to map the annotation (in GFF) of taurine cattle onto the F1 maternal and paternal haplotypes, the F1 primary assembly, and the existing draft assembly. Liftoff was run using "-copies" to look for extra gene copies in the target genome and "-sc 0.95" to specify a minimum sequence identity in exons/CDS of 95% to consider a gene a copy.

Structural variants

We constructed per-chromosome pangenomes with minigraph v0.20 (Li et al., 2020) using "-cxggs -j 0.2" from the five *Bos* and two *Bison* species from the synteny analysis, using the *Bos taurus taurus* reference sequence as backbone and adding assemblies in order of their mash v2.3 divergence (Ondov et al., 2016). Graph paths (P-lines) were reconstructed using minigraph call, allowing vg v1.55.0 deconstruct (Liao et al., 2023) to call structural variants (SV) for each assembly using taurine cattle as reference. We used BCFtools query v1.19 (Danecek et al., 2021) to print genotypes for each SV, which were then plotted with upsetplot v0.9 (https://github.com/jnothman/UpSetPlot). We estimated the SV-tree considering the reciprocal of number of SVs between each pair of assemblies, followed by applying an UPGMA clustering with SciPy v1.12 (Virtanen et al., 2020). The functional impact of SVs was predicted with the Variant Effect Predictor (VEP) tool (McLaren et al., 2016).

Alignment of short-read DNA samples

We supplemented our short-read dataset with previously generated short-read sequencing data of two male wild wisents (BBO_3569 and BBO_3574) (BioProject: PRJNA312492) (Gautier et al., 2016). We also included short-read sequencing data of four American bisons (BioProject: PRJNA343262), and four cattle from European taurine breeds (BioProject: PRJNA176557) (Stothard et al., 2015). For more information about these samples, refer to **Supplementary Table 1**.

The quality of the raw sequencing data was assessed using the FastQC v0.11.9 software (https://www.bioinformatics.babraham.ac.uk/projects/fastqc/). Reads were aligned to our wisent assembly using the MEM algorithm of the Burrows-Wheeler Alignment (BWA) software v0.7.17-r1188 (Li, 2013) with "-T 20" to output only alignments with mapping quality >20. Duplicate reads were marked with samblaster v0.1.24 (Faust and Hall, 2014), and SAMtools v1.19.2 was used to convert the SAM file into a binary BAM format. Sambamba v0.8.1 (Tarasov et al., 2015) was used for coordinate-sorting, and bamtools v2.5.1 (Barnett et al., 2011) and Qualimap v2.3 (Okonechnikov et al., 2016) were used to assess the quality of the alignments. Reads were also aligned to the ARS-UCD1.2 assembly.

Variant calling, postfiltering, and statistics

Variants were called using Freebayes v0.9.21 (Garrison and Marth, 2012) specifying a minimum base quality of 20, a minimum alternate fraction of 0.20, a minimum alternate count of 2, a haplotype length of 0, and a ploidy level of 2. We used a custom python script by setting to missing individual variants whose depth was <1/3 or >2.5 the average genome coverage, as estimated by Qualimap. BCFtools v1.19 was used to further discard SNPs closer than 5 bp to insertions/deletions (InDels), InDels closer than 5 bp to other InDels, variants with a PHRED-quality score <30, and variants with an

allele count <2. Finally, BCFtools stats was used to obtain statistics on the final set of called variants. Only autosomal bi-allelic SNPs (InDels excluded) were used in the downstream analyses.

Genome-wide heterozygosity

Heterozygosity was calculated in 1 Mb sliding windows as the number of heterozygous bi-allelic SNPs divided by the total number of bases that had >1/3 and <2.5-times the average genome coverage (Bortoluzzi et al., 2020; Bosse et al., 2012). Heterozygosity was corrected for the number of sites that were excluded because of coverage. Windows with less than 60% of bases within a normal coverage range were excluded.

Detecting runs of homozygosity

We identified runs of homozygosity (ROH) using the approach presented in (Bortoluzzi et al., 2020), which uses a corrected measure of heterozygosity estimated in 10 Kb windows (Bosse et al., 2012). The heterozygosity threshold within a candidate ROH was relaxed to allow peaks of heterozygosity if their inclusion did not inflate the heterozygosity within the final ROH, which had to be below 0.25 the average heterozygosity. This minimized the impact of local assembly or alignment errors.

Realized genomic inbreeding

The realized genomic inbreeding coefficient (F_{ROH}) was estimated from the sum of autosomal ROH longer than 100 Kb divided by the genome length of the first 29 autosomes in the wisent genome (L = 2,682,350,267 bp).

Coverage analysis near the *THRSP* deletion

We assessed coverage near the *THRSP* deletion in the six short read-sequenced wisent samples and 719 publicly available short read samples of wisent, bison, taurine, cattle, indicine cattle, and water buffalo aligned to ARS-UCD1.2 with samtools depth with flags "-aa -r 29:17990000-18000000". Accession numbers of the DNA sequencing data are provided in **Supplementary Table 7**. Coverage was normalized based on the mean sequencing depth across this interval, excluding the deletion region (29:17993500-17996000).

Transcriptome analyses

Publicly available RNA sequencing data from bison (BioProject: PRJNA257088, (Dobson et al., 2021)) and water buffalo (BioProject: PRJNA951806, (Si et al., 2023)) were aligned to the ARS-UCD1.2 assembly and Refseq version 106 annotation with STAR v2.7.9a (Dobin et al., 2013). Integrative

Genomics Viewer v2.14.0 (Robinson et al., 2011) was used to visualize the alignments. Accession numbers of the RNA sequencing data are listed in **Supplementary Table 7**. Transcript abundance was quantified using the kallisto v0.46.1 software (Bray et al., 2016). Gene expression from *Bos taurus taurus* transcriptomes was obtained from a publicly available TPM matrix (https://zenodo.org/records/7560235) built by the cattle Genotype-Tissue Expression (GTEx) project (Liu et al., 2022).

Data and resource availability

The primary assembly of the wisent is publicly available in the European Nucleotide Archive (ENA) under accession GCA_963879515.1 (https://www.ebi.ac.uk/ena/browser/view/GCA_963879515.1). The annotation of the primary assembly is currently underway at Ensembl. HiFi reads of the F1 are available in the ENA at the study accession PRJEB71066 under sample accession SAMEA114863253. Illumina paired-end reads of six captive wisents are available in the ENA at the study accession PRJEB71066 under sample accessions SAMEA115388352, SAMEA115388353, SAMEA115388354 (F1), SAMEA115388355 (dam), SAMEA115388356 (sire), SAMEA115388357. Codes used in this study are available in GitHub: https://github.com/cbortoluzzi/WisentGenomeAssembly.

Acknowledgments

We thank Stefan Hoby from the Tierpark Bern and Martin Kilchenmann from the Tierpark Langenberg for providing DNA and tissue samples used in this study. We are thankful for the technical support provided by Dr. Anna Bratus-Neuenschwander from the ETH Zurich technology platform Functional Genomics Center Zurich (https://fgcz.ch) for sequencing and DNA fragment analysis.

Author contributions

CB characterized genomic diversity, identified ROH, analyzed repeats and synteny, built phylogenetic trees, and drafted the paper; XMM prepared DNA for sequencing; SN and FJ sampled tissue; HP conceived the study, examined SV diversity, investigated putative trait-associated SVs, performed transcriptome analyses, and drafted the paper; ASL assembled genomes, investigated the impact of ROH on the assembly process, built and decomposed pangenomes, contributed to the analysis of putative trait-associated SVs, and drafted the paper. All authors read and approved the final manuscript.

Competing Interests

The authors declare that they do not have any conflict of interest to disclose.

Funder Information

This study was supported by the Swiss National Science Foundation (SNSF, grant ID 204654).

References

Adelson, D.L., Raison, J.M., Edgar, R.C., 2009. Characterization and distribution of retrotransposons and simple sequence repeats in the bovine genome. Proc Natl Acad Sci U S A 106, 12855–12860. https://doi.org/10.1073/pnas.0901282106

Alonge, M., Lebeigle, L., Kirsche, M., Jenike, K., Ou, S., Aganezov, S., Wang, X., Lippman, Z.B., Schatz, M.C., Soyk, S., 2022. Automated assembly scaffolding using RagTag elevates a new tomato system for high-throughput genome editing. Genome Biology 23, 258. https://doi.org/10.1186/s13059-022-02823-7

Anderson, G.W., Zhu, Q., Metkowski, J., Stack, M.J., Gopinath, S., Mariash, C.N., 2009. The Thrsp Null Mouse (Thrsptm1cnm) and Diet Induced Obesity. Mol Cell Endocrinol 302, 99–107. https://doi.org/10.1016/j.mce.2009.01.005

Bao, W., Kojima, K.K., Kohany, O., 2015. Repbase Update, a database of repetitive elements in eukaryotic genomes. Mobile DNA 6, 11. https://doi.org/10.1186/s13100-015-0041-9

Bao, Z., Eddy, S.R., 2002. Automated de novo identification of repeat sequence families in sequenced genomes. Genome Res 12, 1269–1276. https://doi.org/10.1101/gr.88502

Barnett, D.W., Garrison, E.K., Quinlan, A.R., Strömberg, M.P., Marth, G.T., 2011. BamTools: a C++ API and toolkit for analyzing and managing BAM files. Bioinformatics 27, 1691–1692. https://doi.org/10.1093/bioinformatics/btr174

Benson, G., 1999. Tandem repeats finder: a program to analyze DNA sequences. Nucleic Acids Res 27, 573–580. https://doi.org/10.1093/nar/27.2.573

Bont, R. de, 2017. Extinct in the Wild: Finding a Place for the European Bison, 1919–1952, in: Spatializing the History of Ecology. Routledge.

Bortoluzzi, C., Bosse, M., Derks, M.F.L., Crooijmans, R.P.M.A., Groenen, M.A.M., Megens, H.-J., 2020. The type of bottleneck matters: Insights into the deleterious variation landscape of small managed populations. Evolutionary Applications 13, 330–341. https://doi.org/10.1111/eva.12872

Bortoluzzi, C., Wright, C.J., Lee, S., Cousins, T., Genez, T.A.L., Thybert, D., Martin, F.J., Haggerty, L., Consortium, T.D.T. of L.P., Blaxter, M., Durbin, R., 2023. Lepidoptera genomics based on 88 chromosomal reference sequences informs population genetic parameters for conservation. https://doi.org/10.1101/2023.04.14.536868

Bosse, M., Megens, H.-J., Madsen, O., Paudel, Y., Frantz, L.A.F., Schook, L.B., Crooijmans, R.P.M.A., Groenen, M.A.M., 2012. Regions of Homozygosity in the Porcine Genome: Consequence of Demography and the Recombination Landscape. PLOS Genetics 8, e1003100. https://doi.org/10.1371/journal.pgen.1003100

Bosse, M., van Loon, S., 2022. Challenges in quantifying genome erosion for conservation. Front Genet 13, 960958. https://doi.org/10.3389/fgene.2022.960958

Bray, N.L., Pimentel, H., Melsted, P., Pachter, L., 2016. Near-optimal probabilistic RNA-seq quantification. Nat Biotech 34, 525–527. https://doi.org/10.1038/nbt.3519

Capella-Gutiérrez, S., Silla-Martínez, J.M., Gabaldón, T., 2009. trimAl: a tool for automated alignment trimming in large-scale phylogenetic analyses. Bioinformatics 25, 1972–1973. https://doi.org/10.1093/bioinformatics/btp348

Chen, L., Qiu, Q., Jiang, Y., Wang, K., Lin, Z., Li, Z., Bibi, F., Yang, Y., Wang, J., Nie, W., Su, W., Liu, G., Li, Q., Fu, W., Pan, X., Liu, C., Yang, J., Zhang, Chenzhou, Yin, Y., Wang, Yu, Zhao, Y., Zhang, Chen, Wang, Z., Qin, Y., Liu, W., Wang, B., Ren, Y., Zhang, R., Zeng, Y., da Fonseca, R.R., Wei, B., Li, R., Wan, W., Zhao, R., Zhu, W., Wang, Yutao, Duan, S., Gao, Y., Zhang, Y.E., Chen, C., Hvilsom, C., Epps, C.W., Chemnick, L.G., Dong, Y., Mirarab, S., Siegismund, H.R., Ryder, O.A., Gilbert, M.T.P., Lewin, H.A., Zhang, G., Heller, R., Wang, W., 2019. Large-scale ruminant genome sequencing provides insights into their evolution and distinct traits. Science 364, eaav6202. https://doi.org/10.1126/science.aav6202

Chen, N.-C., Solomon, B., Mun, T., Iyer, S., Langmead, B., 2021. Reference flow: reducing reference bias using multiple population genomes. Genome Biology 22, 8. https://doi.org/10.1186/s13059-020-02229-3

Cheng, H., Concepcion, G.T., Feng, X., Zhang, H., Li, H., 2021. Haplotype-resolved de novo assembly using phased assembly graphs with hifiasm. Nature Methods 18, 170–175. https://doi.org/10.1038/s41592-020-01056-5

Chu, C., Borges-Monroy, R., Viswanadham, V.V., Lee, S., Li, H., Lee, E.A., Park, P.J., 2021. Comprehensive identification of transposable element insertions using multiple sequencing technologies. Nat Commun 12, 3836. https://doi.org/10.1038/s41467-021-24041-8

Colbert, C.L., Kim, C.-W., Moon, Y.-A., Henry, L., Palnitkar, M., McKean, W.B., Fitzgerald, K., Deisenhofer, J., Horton, J.D., Kwon, H.J., 2010. Crystal structure of Spot 14, a modulator of fatty acid synthesis. Proc Natl Acad Sci U S A 107, 18820–18825. https://doi.org/10.1073/pnas.1012736107

Cordain, L., Watkins, B.A., Florant, G.L., Kelher, M., Rogers, L., Li, Y., 2002. Fatty acid analysis of wild ruminant tissues: evolutionary implications for reducing diet-related chronic disease. Eur J Clin Nutr 56, 181–191. https://doi.org/10.1038/sj.ejcn.1601307

Crysnanto, D., Leonard, A.S., Fang, Z.-H., Pausch, H., 2021. Novel functional sequences uncovered through a bovine multiassembly graph. PNAS 118. https://doi.org/10.1073/pnas.2101056118

Danecek, P., Bonfield, J.K., Liddle, J., Marshall, J., Ohan, V., Pollard, M.O., Whitwham, A., Keane, T., McCarthy, S.A., Davies, R.M., Li, H., 2021. Twelve years of SAMtools and BCFtools. GigaScience 10, giab008. https://doi.org/10.1093/gigascience/giab008

Dobin, A., Davis, C.A., Schlesinger, F., Drenkow, J., Zaleski, C., Jha, S., Batut, P., Chaisson, M., Gingeras, T.R., 2013. STAR: ultrafast universal RNA-seq aligner. Bioinformatics 29, 15–21. https://doi.org/10.1093/bioinformatics/bts635

Dobson, L.K., Zimin, A., Bayles, D., Fritz-Waters, E., Alt, D., Olsen, S., Blanchong, J., Reecy, J., Smith, T.P.L., Derr, J.N., 2021. De novo assembly and annotation of the North American bison (Bison bison) reference genome and subsequent variant identification. Anim Genet 52, 263–274. https://doi.org/10.1111/age.13060

Druet, T., Oleński, K., Flori, L., Bertrand, A.R., Olech, W., Tokarska, M., Kaminski, S., Gautier, M., 2020. Genomic Footprints of Recovery in the European Bison. Journal of Heredity 111, 194–203. https://doi.org/10.1093/jhered/esaa002

Faust, G.G., Hall, I.M., 2014. SAMBLASTER: fast duplicate marking and structural variant read extraction. Bioinformatics 30, 2503–2505. https://doi.org/10.1093/bioinformatics/btu314

Flynn, J.M., Hubley, R., Goubert, C., Rosen, J., Clark, A.G., Feschotte, C., Smit, A.F., 2020. RepeatModeler2 for automated genomic discovery of transposable element families. Proceedings of the National Academy of Sciences 117, 9451–9457. https://doi.org/10.1073/pnas.1921046117

Garrison, E., Marth, G., 2012. Haplotype-based variant detection from short-read sequencing. https://doi.org/10.48550/arXiv.1207.3907

Gautier, M., Moazami-Goudarzi, K., Levéziel, H., Parinello, H., Grohs, C., Rialle, S., Kowalczyk, R., Flori, L., 2016. Deciphering the Wisent Demographic and Adaptive Histories from Individual Whole-Genome Sequences. Molecular Biology and Evolution 33, 2801–2814. https://doi.org/10.1093/molbev/msw144

Günther, T., Nettelblad, C., 2019. The presence and impact of reference bias on population genomic studies of prehistoric human populations. PLOS Genetics 15, e1008302. https://doi.org/10.1371/journal.pgen.1008302

Guy, L., Kultima, J.R., Andersson, S.G.E., 2010. genoPlotR: comparative gene and genome visualization in R. Bioinformatics 26, 2334–2335. https://doi.org/10.1093/bioinformatics/btq413

Huang, N., Li, H., 2023. compleasm: a faster and more accurate reimplementation of BUSCO. Bioinformatics 39, btad595. https://doi.org/10.1093/bioinformatics/btad595

Jarvis, E.D., Formenti, G., Rhie, A., Guarracino, A., Yang, C., Wood, J., Tracey, A., Thibaud-Nissen, F., Vollger, M.R., Porubsky, D., Cheng, H., Asri, M., Logsdon, G.A., Carnevali, P., Chaisson, M.J.P., Chin, C.-S., Cody, S., Collins, J., Ebert, P., Escalona, M., Fedrigo, O., Fulton, R.S., Fulton, L.L., Garg, S., Gerton, J.L., Ghurye, J., Granat, A., Green, R.E., Harvey, W., Hasenfeld, P., Hastie, A., Haukness, M., Jaeger, E.B., Jain, M., Kirsche, M., Kolmogorov, M., Korbel, J.O., Koren, S., Korlach, J., Lee, J., Li, D., Lindsay, T., Lucas, J., Luo, F., Marschall, T., Mitchell, M.W., McDaniel, J., Nie, F., Olsen, H.E., Olson, N.D., Pesout, T., Potapova, T., Puiu, D., Regier, A.,

Ruan, J., Salzberg, S.L., Sanders, A.D., Schatz, M.C., Schmitt, A., Schneider, V.A., Selvaraj, S., Shafin, K., Shumate, A., Stitziel, N.O., Stober, C., Torrance, J., Wagner, J., Wang, J., Wenger, A., Xiao, C., Zimin, A.V., Zhang, G., Wang, T., Li, H., Garrison, E., Haussler, D., Hall, I., Zook, J.M., Eichler, E.E., Phillippy, A.M., Paten, B., Howe, K., Miga, K.H., 2022. Semi-automated assembly of high-quality diploid human reference genomes. Nature 611, 519–531. https://doi.org/10.1038/s41586-022-05325-5

Katoh, K., Standley, D.M., 2013. MAFFT multiple sequence alignment software version 7: improvements in performance and usability. Mol Biol Evol 30, 772–780. https://doi.org/10.1093/molbev/mst010

Koch, R.M., Jung, H.G., Crouse, J.D., Varel, V.H., Cundiff, L.V., 1995. Growth, digestive capability, carcass, and meat characteristics of Bison bison, Bos taurus, and Bos x Bison. J Anim Sci 73, 1271–1281. https://doi.org/10.2527/1995.7351271x

Koren, S., Rhie, A., Walenz, B.P., Dilthey, A.T., Bickhart, D.M., Kingan, S.B., Hiendleder, S., Williams, J.L., Smith, T.P.L., Phillippy, A.M., 2018. *De novo* assembly of haplotype-resolved genomes with trio binning. Nature Biotechnology 36, 1174–1182. https://doi.org/10.1038/nbt.4277

Koren, S., Walenz, B.P., Berlin, K., Miller, J.R., Bergman, N.H., Phillippy, A.M., 2017. Canu: scalable and accurate long-read assembly via adaptive k-mer weighting and repeat separation. Genome Res. 27, 722–736. https://doi.org/10.1101/gr.215087.116

Kuemmerle, N.B., Kinlaw, W.B., 2011. THRSP (thyroid hormone responsive). Atlas Genet Cytogenet Oncol Haematol 15, 480–482.

LaFave, L.T., Augustin, L.B., Mariash, C.N., 2006. S14: insights from knockout mice. Endocrinology 147, 4044–4047. https://doi.org/10.1210/en.2006-0473

Leonard, A.S., Crysnanto, D., Fang, Z.-H., Heaton, M.P., Vander Ley, B.L., Herrera, C., Bollwein, H., Bickhart, D.M., Kuhn, K.L., Smith, T.P.L., Rosen, B.D., Pausch, H., 2022. Structural variant-based pangenome construction has low sensitivity to variability of haplotype-resolved bovine assemblies. Nat Commun 13, 3012. https://doi.org/10.1038/s41467-022-30680-2

Leonard, A.S., Crysnanto, D., Mapel, X.M., Bhati, M., Pausch, H., 2023. Graph construction method impacts variation representation and analyses in a bovine super-pangenome. Genome Biol 24, 124. https://doi.org/10.1186/s13059-023-02969-y

Leonard, A.S., Mapel, X.M., Pausch, H., 2024. Pangenome genotyped structural variation improves molecular phenotype mapping in cattle. Genome Res. gr.278267.123. https://doi.org/10.1101/gr.278267.123

Li, H., 2018. Minimap2: pairwise alignment for nucleotide sequences. Bioinformatics 34, 3094–3100. https://doi.org/10.1093/bioinformatics/bty191

Li, H., 2013. Aligning sequence reads, clone sequences and assembly contigs with BWA-MEM. arXiv:1303.3997 [q-bio].

Li, H., Feng, X., Chu, C., 2020. The design and construction of reference pangenome graphs with minigraph. Genome Biology 21, 265. https://doi.org/10.1186/s13059-020-02168-z

Li, H., Handsaker, B., Wysoker, A., Fennell, T., Ruan, J., Homer, N., Marth, G., Abecasis, G., Durbin, R., 2009. The Sequence Alignment/Map format and SAMtools. Bioinformatics 25, 2078–2079. https://doi.org/10.1093/bioinformatics/btp352

Liao, W.-W., Asri, M., Ebler, J., Doerr, D., Haukness, M., Hickey, G., Lu, S., Lucas, J.K., Monlong, J., Abel, H.J., Buonaiuto, S., Chang, X.H., Cheng, H., Chu, J., Colonna, V., Eizenga, J.M., Feng, X., Fischer, C., Fulton, R.S., Garg, S., Groza, C., Guarracino, A., Harvey, W.T., Heumos, S., Howe, K., Jain, M., Lu, T.-Y., Markello, C., Martin, F.J., Mitchell, M.W., Munson, K.M., Mwaniki, M.N., Novak, A.M., Olsen, H.E., Pesout, T., Porubsky, D., Prins, P., Sibbesen, J.A., Sirén, J., Tomlinson, C., Villani, F., Vollger, M.R., Antonacci-Fulton, L.L., Baid, G., Baker, C.A., Belyaeva, A., Billis, K., Carroll, A., Chang, P.-C., Cody, S., Cook, D.E., Cook-Deegan, R.M., Cornejo, O.E., Diekhans, M., Ebert, P., Fairley, S., Fedrigo, O., Felsenfeld, A.L., Formenti, G., Frankish, A., Gao, Y., Garrison, N.A., Giron, C.G., Green, R.E., Haggerty, L., Hoekzema, K., Hourlier, T., Ji, H.P., Kenny, E.E., Koenig, B.A., Kolesnikov, A., Korbel, J.O., Kordosky, J., Koren, S., Lee, H., Lewis, A.P., Magalhães, H., Marco-Sola, S., Marijon, P., McCartney, A., McDaniel, J., Mountcastle, J., Nattestad, M., Nurk, S., Olson, N.D., Popejoy, A.B., Puiu, D., Rautiainen, M., Regier, A.A., Rhie, A., Sacco, S., Sanders, A.D., Schneider, V.A., Schultz, B.I., Shafin, K., Smith, M.W., Sofia, H.J., Abou Tayoun, A.N., Thibaud-Nissen, F., Tricomi, F.F., Wagner, J., Walenz, B., Wood, J.M.D., Zimin, A.V., Bourque, G., Chaisson, M.J.P., Flicek, P., Phillippy, A.M., Zook, J.M., Eichler, E.E., Haussler, D., Wang, T., Jarvis, E.D., Miga, K.H., Garrison, E., Marschall, T., Hall, I.M., Li, H., Paten, B., 2023. A draft human pangenome reference. Nature 617, 312–324. https://doi.org/10.1038/s41586-023-05896-x

Liu, S., Gao, Y., Canela-Xandri, O., Wang, S., Yu, Y., Cai, W., Li, B., Xiang, R., Chamberlain, A.J., Pairo-Castineira, E., D'Mellow, K., Rawlik, K., Xia, C., Yao, Y., Navarro, P., Rocha, D., Li, X., Yan, Z., Li, C., Rosen, B.D., Van Tassell, C.P., Vanraden, P.M., Zhang, S., Ma, L., Cole, J.B., Liu, G.E., Tenesa, A., Fang, L., 2022. A multi-tissue atlas of regulatory variants in cattle. Nat Genet 54, 1438–1447. https://doi.org/10.1038/s41588-022-01153-5

Mastromonaco, G.F., Coppola, G., Crawshaw, G., DiBerardino, D., King, W.A., 2004. Identification of the homologue of the bovine Rob(1;29) in a captive gaur (Bos gaurus). Chromosome Res 12, 725–731. https://doi.org/10.1023/B:CHRO.0000045800.44911.67

McLaren, W., Gil, L., Hunt, S.E., Riat, H.S., Ritchie, G.R.S., Thormann, A., Flicek, P., Cunningham, F., 2016. The Ensembl Variant Effect Predictor. Genome Biology 17, 122. https://doi.org/10.1186/s13059-016-0974-4

Milia, S., Leonard, A.S., Mapel, X.M., Ulloa, S.M.B., Drögemüller, C., Pausch, H., 2024. Taurine pangenome uncovers a segmental duplication upstream of KIT associated with depigmentation in white-headed cattle. https://doi.org/10.1101/2024.02.02.578587

Okonechnikov, K., Conesa, A., García-Alcalde, F., 2016. Qualimap 2: advanced multi-sample quality control for high-throughput sequencing data. Bioinformatics 32, 292–294. https://doi.org/10.1093/bioinformatics/btv566

Olech, W., Perzanowski, K., 2022. European Bison Species Strategic Review – perspectives and challenges. European Bison Conservation Newsletter 14, 5–10.

Ondov, B.D., Treangen, T.J., Melsted, P., Mallonee, A.B., Bergman, N.H., Koren, S., Phillippy, A.M., 2016. Mash: fast genome and metagenome distance estimation using MinHash. Genome Biology 17, 132. https://doi.org/10.1186/s13059-016-0997-x

Oppenheimer, J., Rosen, B.D., Heaton, M.P., Vander Ley, B.L., Shafer, W.R., Schuetze, F.T., Stroud, B., Kuehn, L.A., McClure, J.C., Barfield, J.P., Blackburn, H.D., Kalbfleisch, T.S., Bickhart, D.M., Davenport, K.M., Kuhn, K.L., Green, R.E., Shapiro, B., Smith, T.P.L., 2021. A Reference Genome Assembly of American Bison, Bison bison bison. Journal of Heredity 112, 174–183. https://doi.org/10.1093/jhered/esab003

Plumb, G., 2022. A range-wide conservation action plan for the European bison. Oryx 56, 171–171. https://doi.org/10.1017/S003060532100185X

Price, A.L., Jones, N.C., Pevzner, P.A., 2005. De novo identification of repeat families in large genomes. Bioinformatics 21 Suppl 1, i351-358. https://doi.org/10.1093/bioinformatics/bti1018

Rhie, A., Walenz, B.P., Koren, S., Phillippy, A.M., 2020. Merqury: reference-free quality, completeness, and phasing assessment for genome assemblies. Genome Biology 21, 245. https://doi.org/10.1186/s13059-020-02134-9

Rice, E.S., Koren, S., Rhie, A., Heaton, M.P., Kalbfleisch, T.S., Hardy, T., Hackett, P.H., Bickhart, D.M., Rosen, B.D., Ley, B.V., Maurer, N.W., Green, R.E., Phillippy, A.M., Petersen, J.L., Smith, T.P.L., 2020. Continuous chromosome-scale haplotypes assembled from a single interspecies F1 hybrid of yak and cattle. GigaScience 9, giaa029. https://doi.org/10.1093/gigascience/giaa029

Robinson, J.T., Thorvaldsdóttir, H., Winckler, W., Guttman, M., Lander, E.S., Getz, G., Mesirov, J.P., 2011. Integrative Genomics Viewer. Nat Biotechnol 29, 24–26. https://doi.org/10.1038/nbt.1754

Rule, D.C., Broughton, K.S., Shellito, S.M., Maiorano, G., 2002. Comparison of muscle fatty acid profiles and cholesterol concentrations of bison, beef cattle, elk, and chicken. J Anim Sci 80, 1202–1211. https://doi.org/10.2527/2002.8051202x

Schering, L., Albrecht, E., Komolka, K., Kühn, C., Maak, S., 2017. Increased expression of thyroid hormone responsive protein (THRSP) is the result but not the cause of higher intramuscular fat content in cattle. Int J Biol Sci 13, 532–544. https://doi.org/10.7150/ijbs.18775

Shumate, A., Salzberg, S.L., 2021. Liftoff: accurate mapping of gene annotations. Bioinformatics 37, 1639–1643. https://doi.org/10.1093/bioinformatics/btaa1016

Si, J., Dai, D., Li, K., Fang, L., Zhang, Y., 2023. A Multi-Tissue Gene Expression Atlas of Water Buffalo (Bubalus bubalis) Reveals Transcriptome Conservation between Buffalo and Cattle. Genes 14, 890. https://doi.org/10.3390/genes14040890

Smith, T.P.L., Bickhart, D.M., Boichard, D., Chamberlain, A.J., Djikeng, A., Jiang, Y., Low, W.Y., Pausch, H., Demyda-Peyrás, S., Prendergast, J., Schnabel, R.D., Rosen, B.D., Bovine Pangenome Consortium, 2023. The Bovine Pangenome Consortium: democratizing production and accessibility of genome assemblies for global cattle breeds and other bovine species. Genome Biology 24, 139. https://doi.org/10.1186/s13059-023-02975-0

Soubrier, J., Gower, G., Chen, K., Richards, S.M., Llamas, B., Mitchell, K.J., Ho, S.Y.W., Kosintsev, P., Lee, M.S.Y., Baryshnikov, G., Bollongino, R., Bover, P., Burger, J., Chivall, D., Crégut-Bonnoure, E., Decker, J.E., Doronichev, V.B., Douka, K., Fordham, D.A., Fontana, F., Fritz, C.,

Glimmerveen, J., Golovanova, L.V., Groves, C., Guerreschi, A., Haak, W., Higham, T., Hofman-Kamińska, E., Immel, A., Julien, M.-A., Krause, J., Krotova, O., Langbein, F., Larson, G., Rohrlach, A., Scheu, A., Schnabel, R.D., Taylor, J.F., Tokarska, M., Tosello, G., van der Plicht, J., van Loenen, A., Vigne, J.-D., Wooley, O., Orlando, L., Kowalczyk, R., Shapiro, B., Cooper, A., 2016. Early cave art and ancient DNA record the origin of European bison. Nat Commun 7, 13158. https://doi.org/10.1038/ncomms13158

Stamatakis, A., 2014. RAxML version 8: a tool for phylogenetic analysis and post-analysis of large phylogenies. Bioinformatics 30, 1312–1313. https://doi.org/10.1093/bioinformatics/btu033

Stothard, P., Liao, X., Arantes, A.S., De Pauw, M., Coros, C., Plastow, G.S., Sargolzaei, M., Crowley, J.J., Basarab, J.A., Schenkel, F., Moore, S., Miller, S.P., 2015. A large and diverse collection of bovine genome sequences from the Canadian Cattle Genome Project. GigaScience 4, 49. https://doi.org/10.1186/s13742-015-0090-5

Stroupe, S., Forgacs, D., Harris, A., Derr, J.N., Davis, B.W., 2022. Genomic evaluation of hybridization in historic and modern North American Bison (Bison bison). Sci Rep 12, 6397. https://doi.org/10.1038/s41598-022-09828-z

Stroupe, S., Martone, C., McCann, B., Juras, R., Kjöllerström, H.J., Raudsepp, T., Beard, D., Davis, B.W., Derr, J.N., 2023. Chromosome-level reference genome for North American bison (Bison bison) and variant database aids in identifying albino mutation. G3 Genes|Genomes|Genetics 13, jkad156. https://doi.org/10.1093/g3journal/jkad156

Tarasov, A., Vilella, A.J., Cuppen, E., Nijman, I.J., Prins, P., 2015. Sambamba: fast processing of NGS alignment formats. Bioinformatics 31, 2032–2034. https://doi.org/10.1093/bioinformatics/btv098

Thomma, B.P.H.J., Seidl, M.F., Shi-Kunne, X., Cook, D.E., Bolton, M.D., van Kan, J.A.L., Faino, L., 2016. Mind the gap; seven reasons to close fragmented genome assemblies. Fungal Genet Biol 90, 24–30. https://doi.org/10.1016/j.fgb.2015.08.010

Tokarska, M., Marshall, T., Kowalczyk, R., Wójcik, J.M., Pertoldi, C., Kristensen, T.N., Loeschcke, V., Gregersen, V.R., Bendixen, C., 2009. Effectiveness of microsatellite and SNP markers for parentage and identity analysis in species with low genetic diversity: the case of European bison. Heredity (Edinb) 103, 326–332. https://doi.org/10.1038/hdy.2009.73

Tokarska, M., Pertoldi, C., Kowalczyk, R., Perzanowski, K., 2011. Genetic status of the European bison Bison bonasus after extinction in the wild and subsequent recovery. Mammal Review 41, 151–162. https://doi.org/10.1111/j.1365-2907.2010.00178.x

Tonkin-Hill, G., MacAlasdair, N., Ruis, C., Weimann, A., Horesh, G., Lees, J.A., Gladstone, R.A., Lo, S., Beaudoin, C., Floto, R.A., Frost, S.D.W., Corander, J., Bentley, S.D., Parkhill, J., 2020. Producing polished prokaryotic pangenomes with the Panaroo pipeline. Genome Biology 21, 180. https://doi.org/10.1186/s13059-020-02090-4

Virtanen, P., Gommers, R., Oliphant, T.E., Haberland, M., Reddy, T., Cournapeau, D., Burovski, E., Peterson, P., Weckesser, W., Bright, J., van der Walt, S.J., Brett, M., Wilson, J., Millman, K.J., Mayorov, N., Nelson, A.R.J., Jones, E., Kern, R., Larson, E., Carey, C.J., Polat, İ., Feng, Y., Moore, E.W., VanderPlas, J., Laxalde, D., Perktold, J., Cimrman, R., Henriksen, I., Quintero, E.A., Harris, C.R., Archibald, A.M., Ribeiro, A.H., Pedregosa, F., van Mulbregt, P., 2020. SciPy

1.0: fundamental algorithms for scientific computing in Python. Nat Methods 17, 261–272. https://doi.org/10.1038/s41592-019-0686-2

Wang, K., Wang, L., Lenstra, J.A., Jian, J., Yang, Y., Hu, Q., Lai, D., Qiu, Q., Ma, T., Du, Z., Abbott, R., Liu, J., 2017. The genome sequence of the wisent (Bison bonasus). Gigascience 6, 1–5. https://doi.org/10.1093/gigascience/gix016

Wang, X., Carre, W., Zhou, H., Lamont, S.J., Cogburn, L.A., 2004. Duplicated Spot 14 genes in the chicken: characterization and identification of polymorphisms associated with abdominal fat traits. Gene 332, 79–88. https://doi.org/10.1016/j.gene.2004.02.021

Wang, Y.H., Bower, N.I., Reverter, A., Tan, S.H., De Jager, N., Wang, R., McWilliam, S.M., Cafe, L.M., Greenwood, P.L., Lehnert, S.A., 2009. Gene expression patterns during intramuscular fat development in cattle. J Anim Sci 87, 119–130. https://doi.org/10.2527/jas.2008-1082

Wheeler, T.J., Clements, J., Eddy, S.R., Hubley, R., Jones, T.A., Jurka, J., Smit, A.F.A., Finn, R.D., 2013. Dfam: a database of repetitive DNA based on profile hidden Markov models. Nucleic Acids Res 41, D70–D82. https://doi.org/10.1093/nar/gks1265

Wick, R.R., Schultz, M.B., Zobel, J., Holt, K.E., 2015. Bandage: interactive visualization of de novo genome assemblies. Bioinformatics 31, 3350–3352. https://doi.org/10.1093/bioinformatics/btv383

Wojciechowska, M., Puchała, K., Nowak-Życzyńska, Z., Perlińska-Teresiak, M., Kloch, M., Drobik-Czwarno, W., Olech, W., 2023. From Wisent to the Lab and Back Again—A Complex SNP Set for Population Management as an Effective Tool in European Bison Conservation. Diversity 15, 116. https://doi.org/10.3390/d15010116

Wu, D.-D., Ding, X.-D., Wang, S., Wójcik, J.M., Zhang, Y., Tokarska, M., Li, Y., Wang, M.-S., Faruque, O., Nielsen, R., Zhang, Q., Zhang, Y.-P., 2018. Pervasive introgression facilitated domestication and adaptation in the Bos species complex. Nat Ecol Evol 2, 1139–1145. https://doi.org/10.1038/s41559-018-0562-y